The diurnal cycle of cloud profiles over land and ocean between 51°S and 51°N, seen by the CATS spaceborne lidar from the International Space Station

Vincent Noël, Hélène Chepfer, Marjolaine Chiriaco, John Yorks

Atmos. Chem. Phys., 18, 9457–9473, 2018
https://doi.org/10.5194/acp-18-9457-2018

Atmospheric Chemistry and Physics
Open Access
EGU

The diurnal cycle of cloud profiles over land and ocean between 51° S and 51° N, seen by the CATS spaceborne lidar from the International Space Station

Vincent Noel[1], **Hélène Chepfer**[2], **Marjolaine Chiriaco**[3], **and John Yorks**[4]

[1]Laboratoire d'Aérologie, CNRS/UPS, Observatoire Midi-Pyrénées, 14 avenue Edouard Belin, Toulouse, France
[2]LMD/IPSL, Sorbonne Université, École polytechnique, École Normale Supérieure, PSL Research University, CNRS, 91120 Palaiseau, France
[3]LATMOS/IPSL, Univ. Versailles Saint-Quentin en Yvelines, Guyancourt, France
[4]NASA GSFC, Greenbelt, Maryland, USA

Correspondence: Vincent Noel (vincent.noel@aero.obs-mip.fr)

Received: 27 February 2018 – Discussion started: 26 March 2018
Revised: 19 June 2018 – Accepted: 22 June 2018 – Published: 6 July 2018

Abstract. We document, for the first time, how detailed vertical profiles of cloud fraction (CF) change diurnally between 51° S and 51° N, by taking advantage of 15 months of measurements from the Cloud-Aerosol Transport System (CATS) lidar on the non-sun-synchronous International Space Station (ISS).

Over the tropical ocean in summer, we find few high clouds during daytime. At night they become frequent over a large altitude range (11–16 km between 22:00 and 04:00 LT). Over the summer tropical continents, but not over ocean, CATS observations reveal mid-level clouds (4–8 km above sea level or a.s.l.) persisting all day long, with a weak diurnal cycle (minimum at noon). Over the Southern Ocean, diurnal cycles appear for the omnipresent low-level clouds (minimum between noon and 15:00) and high-altitude clouds (minimum between 08:00 and 14:00). Both cycles are time shifted, with high-altitude clouds following the changes in low-altitude clouds by several hours. Over all continents at all latitudes during summer, the low-level clouds develop upwards and reach a maximum occurrence at about 2.5 km a.s.l. in the early afternoon (around 14:00).

Our work also shows that (1) the diurnal cycles of vertical profiles derived from CATS are consistent with those from ground-based active sensors on a local scale, (2) the cloud profiles derived from CATS measurements at local times of 01:30 and 13:30 are consistent with those observed from CALIPSO at similar times, and (3) the diurnal cycles of low and high cloud amounts (CAs) derived from CATS are in general in phase with those derived from geostationary imagery but less pronounced. Finally, the diurnal variability of cloud profiles revealed by CATS strongly suggests that CALIPSO measurements at 01:30 and 13:30 document the daily extremes of the cloud fraction profiles over ocean and are more representative of daily averages over land, except at altitudes above 10 km where they capture part of the diurnal variability. These findings are applicable to other instruments with local overpass times similar to CALIPSO's, such as all the other A-Train instruments and the future EarthCARE mission.

1 Introduction

The diurnal cycle of clouds has been documented for decades by ground-based instruments (e.g., Gray and Jacobson, 1977) and geostationary satellites (e.g., Rossow, 1989). Even though climatologies give priority to how clouds change with seasons and geography, many studies noted the strong diurnal cycle of boundary layer clouds. During the day, low clouds form in the morning and expand, following the warming of the surface by incoming solar radiation (Stubenrauch et al., 2006). The maximum low cloud amount (CA) is often reached in the early afternoon. This sun-driven variation reaches a maximum over continents, where it depends on orography (Wilson and Barros, 2017; Shang et al., 2018), and in summer. It is more limited over ocean and during winter

(Rozendaal et al., 1995; Soden, 2000). When night falls, condensation in the boundary layer can create stratiform clouds, which stabilize and expand through nighttime radiative cooling at cloud top and reach maximal cover in the early morning (Greenwald and Christopher, 1999; Eastman and Warren, 2014).

In the tropics, the near-surface daily increase in water vapor triggered by solar warming (Tian et al., 2004) is transmitted to higher altitudes through deep convection (Johnson et al., 1999). This imposes a diurnal cycle to high clouds, which is delayed by several hours compared to low clouds (Soden, 2000). Their maximum amount is reached in the evening (Rossow and Schiffer, 1999; Stubenrauch et al., 2006). At midlatitudes, without deep convection most of the troposphere is free from surface influence (Wang and Sassen, 2001), and diurnal changes in the distribution of high-altitude clouds are limited. Changes are rather driven by the local atmospheric circulation (e.g., storm tracks), leading to less predictable patterns which are more location dependent.

More recently, geostationary imagery documented the diurnal variations in the composition of cloud cover above Central Africa (Philippon et al., 2016) and cloud top temperatures (Taylor et al., 2017). In any case, the vertically integrated nature of passive imagery means it cannot resolve the vertical variability of clouds and its diurnal cycle, which is key to better understanding the atmospheric heating rate profile (L'Ecuyer et al., 2008). By comparison, active remote sensing instruments, such as radars and lidars, document the cloud vertical distribution with great accuracy and vertical resolutions finer than 500 m. Long-running datasets from active instruments operated from ground-based sites have led to useful time series and statistics about clouds (e.g., Sassen and Benson, 2001; Hogan et al., 2003; Protat et al., 2009; Dong et al., 2010; Hoareau et al., 2013; Zhao et al., 2017). From space, Liu and Zipser (2008) were able to derive information on the cloud diurnal cycle from the spaceborne Tropical Rainfall Measuring Mission radar, launched in 1997 (Kummerow et al., 1998), but the instrument was not designed to detect clouds with accuracy. The CALIPSO lidar (Cloud-Aerosol Lidar and Infrared Pathfinder Satellite Observations), since its launch into orbit in 2006 (Winker et al., 2010), has provided transformative vertically resolved data on clouds (Stephens et al., 2018; Winker et al., 2017). Cloud detections from CALIPSO have, among other things, helped pinpoint and improve significant cloud-related weaknesses in climate models (e.g., Cesana and Chepfer, 2013; Konsta et al., 2016), helped improve estimates of the surface radiation budget (Kato et al., 2011), and helped improve estimates of the heating rate profile (Haynes et al., 2013; Bouniol et al., 2016). Due to its sun-synchronous polar orbit, CALIPSO samples the atmosphere at either 01:30 or 13:30 local time (LT), similar to the CloudSat radar (Stephens and Kummerow, 2007) and all A-Train instruments (L'Ecuyer and Jiang, 2010). Even though measurements at two times of the day can offer insights into the day–night cloud changes (Sèze et al., 2014; Gupta et al., 2018), they are insufficient to fully document the diurnal evolution of cloud profiles. This observational blind spot explains why very little is known so far about how the vertical distribution of clouds changes diurnally in most of the globe, leading to inconsistencies amongst climate models (Yin and Porporato, 2017).

Here we take advantage of measurements from the Cloud-Aerosol Transport System (CATS, McGill et al., 2015) lidar on the International Space Station (ISS) to document the diurnal evolution of the vertical distribution of clouds in regions of the globe. As the ISS orbits the Earth many times a day between 51° S and 51° N, CATS measurements cannot track the evolution of individual clouds over a given location and a given day. Instead, cloud detections over a given location at variable times of day can be aggregated over seasons to create statistics that eventually document the seasonal average diurnal cycle of clouds over that location. Thus far, the CATS dataset is the only one to contain active vertically resolved measurements made from satellites with variable local times of overpass.

We first describe how data were selected and processed to derive diurnal cycles of cloud fraction (CF) profiles and cloud amounts (CA) from CATS and all other instruments included for comparison (Sect. 2). Then, using CATS retrievals, we document, for the first time, the diurnal cycle of detailed cloud fraction profiles in large regions of the globe in two seasons over ocean and land (Sect. 3.1 and 3.2). In Sect. 3.3 we describe CATS-derived diurnal cycles of cloud profiles over selected sites and continents with two goals in mind: (i) to compare them with independent ground-based observations to check the validity of the CATS retrievals and (ii) to document the diversity of the continental cloud profile diurnal cycles over the globe. In Sect. 4 we discuss implications of our results: we compare the diurnal cycle of the low and high cloud covers derived from CATS with ones from geostationary satellites (Sect. 4.1) and discuss the agreement between CATS cloud fraction profiles derived at the times of CALIPSO overpass with actual CALIPSO retrievals (Sect. 4.2.1). Finally, we consider CATS profiles at overpass times from current and future sun-synchronous spaceborne lidar missions (Sect. 4.2.2) to understand which part of the diurnal cloud cycle is sampled by these instruments. We conclude in Sect. 5.

2 Data and methods

2.1 Data

2.1.1 Cloud detections from the CATS spaceborne lidar

In this study, our primary data consist of clouds detected during June–July–August (JJA) and December–January–February (DJF) periods using data from the CATS lidar system (Yorks et al., 2018). CATS operated from the ISS be-

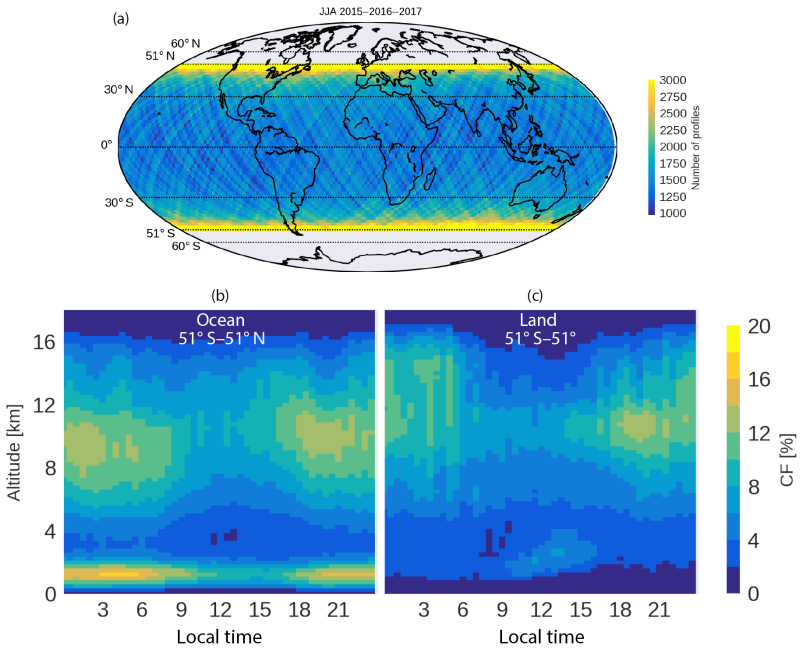

Figure 1. (a) Number of CATS profiles in 2° × 2° longitude–latitude boxes sampled during JJA 2015–2016–2017, with unsampled latitudes in grey. **(b, c)** Evolution of the vertical profile of cloud fraction as a function of local time of observation over the ocean **(b)** and land **(c)**, using CATS detections made in JJA from 2015 to 2017.

tween February 2015 and late October 2017. Although CATS was originally designed to operate at three wavelengths (355, 532 and 1064 nm) with variable viewing geometries, beginning in March 2015 technical issues limited operation to a single 1064 nm wavelength and a single viewing mode. The CATS instrument went on providing single-channel high-quality data (Yorks et al., 2016a) until a fault in the onboard power and data system ended science operations on 30 October 2017.

Being located on the ISS means measurements from CATS are constrained to latitudes below 51°, giving it access to ∼ 78 % of the Earth's surface (Fig. 1, top). This prevents our study from covering polar regions, but leads to densely distributed overpasses at latitudes above 40°. CATS sampling is particularly good in populated midlatitude regions and above the Southern Ocean.

CATS reports vertical profiles of attenuated total backscatter (ATB) every 350 m at 1064 nm with a 60 m vertical resolution (Yorks et al., 2016a). In mode 7.2, in which CATS operates since February 2015, each profile is created by accumulating backscattered energy from 200 4 kHz pulses, 20 times per second. The CATS vertical feature mask algorithms use these calibrated ATB profiles, averaged to 5 and 60 km, to detect atmospheric layers, discriminate clouds from aerosols, and determine cloud phase (Yorks et al., 2016b, 2018). The CATS layer-detection algorithms are based on a threshold-profile technique similar to the one used for CALIOP (Cloud-Aerosol Lidar with Orthogonal Polarization; Vaughan et al., 2009) but, unlike for CALIOP, they rely primarily on 1064 nm ATB (Yorks et al., 2016b). The CATS cloud–aerosol discrimination algorithm uses a probability density function technique that is based on the CALIPSO algorithm but relies on horizontal persistence tests to differentiate between low-level clouds and aerosol because backscatter color ratio, used in the CALIOP algorithms (Liu et al., 2009), is not available in mode 7.2. For cloud phase, CATS uses a layer-integrated 1064 nm depolarization ratio and mid-layer temperature thresholds based on Hu et al. (2009) and Yorks et al. (2011). Minimum horizontal average was 5 km in the nighttime and 60 km in the daytime, a choice that brings the same cloud detection sensitivity to both (Yorks et al., 2016a). This has two consequences: (1) the optically thinnest clouds detected during nighttime at 60 km horizontal averaging might be absent from daytime detections (these represent roughly ∼ 5 % of nighttime clouds) and (2) the horizontal extent and cloud amount of fragmented boundary layer clouds might be overestimated in both daytime and nighttime compared to single-shot detections (as in Chepfer et al., 2013; Cesana et al., 2016). Cloud top and base heights, phase, and other properties are reported in the CATS level 2 operational (L2O) products every 5 km along track. Hereafter, we used such cloud properties from CATS L2O data files v2.01 (Palm et al., 2016), including only layers with a feature type score above 5, to avoid including wrongly classified optically thick aerosol layers near deserts.

To document the diurnal cycle (Sect. 2.2.1), we used CATS cloud detections from JJA and DJF seasons between March 2015 and October 2017. With the CATS cloud data

being still novel at the time of this writing, we document and discuss several of its characteristics in Sects. S1 and S2 in the Supplement, including sampling variability and the sensitivity of cloud detection in the presence of solar pollution. This exploration of CATS data (and the upcoming comparisons with other instruments) made us confident that its sampling and cloud detections are robust enough to be used for scientific purposes.

2.1.2 Cloud detections from ground-based active instruments

As with any lidar, the CATS laser beam becomes fully attenuated when passing through clouds with optical depths larger than typically 3 (e.g., Chepfer et al., 2010). This can lead to the cloud fractions being underestimated in the lower troposphere. Meanwhile, horizontal averaging during daytime can lead to cloud fractions being overestimated at low altitudes. To estimate how much the CATS cloud fraction is biased at low altitudes, we compare CATS detections with independent observations collected from ground-based active instruments.

Ground-based observation sites provide long-term records of atmospheric properties over periods that often cannot be reached by satellite instruments (Chiriaco et al., 2018). Nowadays such sites are often well equipped with active remote sensing instruments. Data acquisition, calibration, and processing are often homogenized in the framework of specific observation networks (e.g., EARLINET, the European Aerosol Research Lidar Network, Pappalardo et al., 2014). Descriptions of the cloud diurnal cycle based on active ground-based measurements are, however, scarce. In this study, we compare CATS cloud cycles with those derived from active measurements at three ground-based sites, two continental, and one oceanic:

- The Site Instrumenté de Recherche par Télédétection Atmosphérique (SIRTA, Haeffelin et al., 2005) is continental, located 20 km southwest of Paris at 48.7° N, 2.2° E. From SIRTA we used cloud detections from the Lidar Nuages et Aérosols (LNA, Elouragini and Flamant, 1996), which were curated, packaged, and made available in the framework of the SIRTA-ReOBS project (Chiriaco et al., 2014, 2018). The LNA requires human supervision and does not operate under precipitation, leading to irregular sampling and almost no nighttime measurements. Thanks to its long operation time, its cloud dataset covers almost 15 years and was used in many studies (e.g., Noel and Haeffelin, 2007; Naud et al., 2010; Dupont et al., 2010). Cloud layers were detected in LNA profiles of attenuated backscatter following a threshold-based approach similar to CATS and CALIPSO.
- The Atmospheric Radiation Measurement (ARM) Southern Great Plains (SGP) site is continental too, at 97° W, 36° N. From ARM-SGP we used the sgparsclkazr1kolliasC1 cloud dataset, which contains vertical cloud detection profiles for every second of every day based on measurements from the 35 GHz Ka ARM zenith radar. This instrument has been operating since 2011 (Kollias et al., 2014). Based on these profiles we reconstructed hourly averages of cloud fraction profiles over seasons during the CATS operation period. Our results closely match those Zhao et al. (2017) derived from the same instrument and those Dupont et al. (2011) derived from the ARM-SGP Raman lidar.
- The ARM Eastern North Atlantic (ENA) site is oceanic, located on Graciosa Island in the Azores archipelago (28.03° W, 39.1° N). From ARM-ENA we used cloud detections from the enaarsclkazr1kolliasC1 dataset derived from a 35 GHz radar similar to the one found at SGP, which we processed in a similar way.

2.1.3 Cloud detections from passive and active spaceborne sensors

In addition to the datasets from CATS, LNA, and two ground-based radars, in the upcoming sections we use cloud retrievals from two spaceborne datasets to put CATS cloud retrievals into a referenced context. First, we consider the baseline reference for the description of the cloud diurnal cycle from space: the analysis of data from the ISCCP done by Rossow and Schiffer (1999), hereafter RS99. Their results are based on aggregated and homogenized infrared and visible radiances from imaging radiometers on the international constellation of weather satellites. They are widely considered to be the reference for describing the diurnal cycle of the cloud cover at large scales from space measurements. We did not reprocess any ISCCP data for the present study; instead we rely on the description of the diurnal cycle of low and high clouds RS99 documented in their Fig. 11 based on ISCCP, to which we compare CATS retrievals in Sect. 4.1.

Finally, we also compare CATS cloud detections with retrievals based on measurements from the CALIOP lidar, routinely made since 2006 from the sun-synchronous CALIPSO platform at 13:30 and 01:30 LT in Sect. 4.2. To enable comparison with CATS retrievals, we used cloud layers retrieved from CALIPSO measurements during the period of CATS operation (March 2015 to October 2017) and documented at a 5 km horizontal resolution in CALIPSO level 2 V4.10 cloud layer products (Vaughan et al., 2009). We processed both CATS and CALIPSO data alike as described in Sect. 2.2.1.

2.2 Methods

2.2.1 Building the diurnal cycle of cloud fraction profiles from lidar cloud detections

Analyzing CATS lidar echoes lets one identify at which altitude a cloud is present above a particular location on Earth at a given moment. By aggregating such information over a long period, vertical profiles of cloud fraction can be derived. A CF(z) profile documents at which frequency clouds were observed at the altitude z over a particular location. Cloud fractions are conceptually equivalent to the cloud amounts derived from passive measurements (next section) but vertically resolved with a 60 m resolution.

From CATS level 2 data files, we extract profile-based cloud detections and use the measurement UTC time and coordinates to deduce their local time of observation. Using the resulting list of cloud layer altitudes, coordinates, and local times of detection, we count the number n of clouds detected within half-hour bins of local time, $2° \times 2°$ latitude–longitude boxes, and 200 m altitude bins. We also count the number of valid data points n_0 within those bins. Eventually, we derive the cloud fraction $\mathrm{CF} = \frac{n}{n_0}$, either in individual local time, latitude–longitude, and altitude bin or by aggregating n and n_0 over a selection of bins. Thus, we recreate a statistically accurate representation of the diurnal cycle of cloud fractions profiles, over any location between 51° S and 51° N, through the aggregation over long periods of cloud detections made over that location on different days and local times.

CATS reports cloud layers as opaque when no echo from the surface is found in the profile below a detected cloud, following the same methodology as in Guzman et al. (2017). Below an opaque cloud layer, there is no laser signal left to propagate, and clouds potentially present at lower altitudes will not be sampled by the lidar. To account for this effect, we consider the portions of profiles below an opaque layer unsampled, and they do not count in the number of valid data points n_0. This approach limits the influence of laser attenuation on cloud detections but cannot totally cancel it. For very low clouds (top below 2 km), we make an exception to this rule and consider the lower part of the profile to be cloudy, as we found this creates the best agreement with ground-based observations.

To enable comparisons with CATS CF profiles (Sects. 3.3 and 4.2), we followed a similar approach to build CF profiles using cloud detections from SIRTA-ReOBS and ARM datasets (Sect. 2.1), as well as from CALIPSO level 2 products (Sect. 2.1.3). In both cases, we counted the number of cloud detections and valid (non-attenuated) measurements in hourly local time bins and 200 m altitude bins. For CALIPSO, only the 01:30 and 13:30 time bins were filled.

2.2.2 Building the diurnal cycle of low and high cloud amounts from CATS data

As ISCCP data are based on radiances, clouds therein are characterized according to their retrieved top pressure P as low ($P > 680$ hPa), middle ($440 < P < 680$ hPa), or high ($P < 440$ hPa). To enable a direct ISCCP–CATS comparison, we derived cloud amounts from CATS data for low and high clouds as defined by altitude: low clouds have their top below 4 km a.s.l., high clouds have their base above 7 km, and mid-level clouds are in between. Using the list of cloud layer altitudes, coordinates, and local times of detection derived from CATS detections (Sect. 2.2.1), we count the number of occurrences n' of at least part of one cloud layer in half-hour bins of local time, $2° \times 2°$ latitude–longitude boxes, and the three altitude ranges (0–4, 4–7, and higher than 7 km a.s.l.). We also count the number of occurrences n'_0 that could possibly be reported given the measurements sampled by CATS within each bin, taking into account the existence of opaque layers. Eventually, we derive the cloud amount $\mathrm{CA} = \frac{n'}{n'_0}$ for low-, mid-, and high-altitude cloud layers, either in individual local time and latitude–longitude bin or by aggregating n' and n'_0 over a selection of bins. Like RS99, we separated CATS cloud detections over land and ocean, based on the International Geosphere-Biosphere Programme surface flag present in CATS L2 products on a profile basis (Palm et al., 2016).

3 Results

3.1 Diurnal cloud fraction profiles observed on a global scale

Figure 1 shows the global diurnal cycle revealed by CATS during JJA from March 2015 to October 2017 over ocean and land (bottom left and right). Low and high clouds are clearly separated, with a band of minimum cloudiness in between (near 4 km a.s.l.). Above both surfaces, CATS data show an increase in high clouds during nighttime. Sassen et al. (2009) explain this increase by the infrared radiative cooling of the upper troposphere. The vertical spread of high clouds is most narrow around noon, at which point their apparent base is the highest. These findings are consistent with CALIPSO retrievals (Sassen et al., 2009; Gupta et al., 2018). The vertical evolution in the fraction of sampled atmosphere due to attenuation by atmospheric components, for these diurnal cycles and all that follow, is documented in Sect. S3 in the Supplement.

Significant differences exist between the cloud profile diurnal cycle above land and ocean. Clouds generally extend higher over land during nighttime: high clouds are vertically most frequent near 10 km over ocean, while they extend up to 14 km above continents until 05:00. Over ocean, high clouds appear to rise late in the afternoon (15:00–18:00) and fall

soon thereafter as the sun sets. Land–ocean differences are most striking at low altitudes: over ocean low clouds are present almost all day long between 0 and 2 km a.s.l., with their CF decreasing from a 20 % maximum around 04:00 to ∼ 10 % between 11:00 and 17:00. Over land, low clouds are most significant during daytime: they appear near 2 km a.s.l. at 10:00 and extend upwards to reach 4 km a.s.l. around 16:00. The associated CF remains low, at most 8 %. These planetary boundary layer (PBL) clouds are most certainly associated with turbulence and convection activity occurring near the surface. They disappear after 16:00 without connecting to the higher layers. The clear-sky band (CF < 2 %) near the surface is largest at night (almost 2 km) and thinnest in the late morning.

Over the ocean, CATS detects more low and high clouds during nighttime. This means that the increase in high clouds does not prevent the lidar measurements from faithfully representing at least part of the nocturnal increase in low clouds. During daytime, the decrease in detection sensitivity due to solar pollution could underestimate the retrieved frequency of clouds (low or high). However, CALIPSO cloud detections also reveal a nighttime increase in high clouds, which Sassen et al. (2009) and Gupta et al. (2018) found far too large to be attributed to detection bias from solar noise. Since CATS daytime cloud detection abilities at 1064 nm are at least as good as CALIOP's at 532 nm (Yorks et al., 2016a), it follows that CATS cloud retrievals should provide a reliable qualitative assessment of their diurnal cycle, as comparisons with ground-based measurements will later show (Sect. 3.3). How much solar noise leads to an underestimate of high clouds in CALIOP and CATS datasets still needs to be quantified.

While these seasonal mean results are informative, they mix together unrelated cloud populations from hemispheres with opposite seasons driven by different circulation regimes. We thus describe the daily cycles of clouds in zonal bands in the next section.

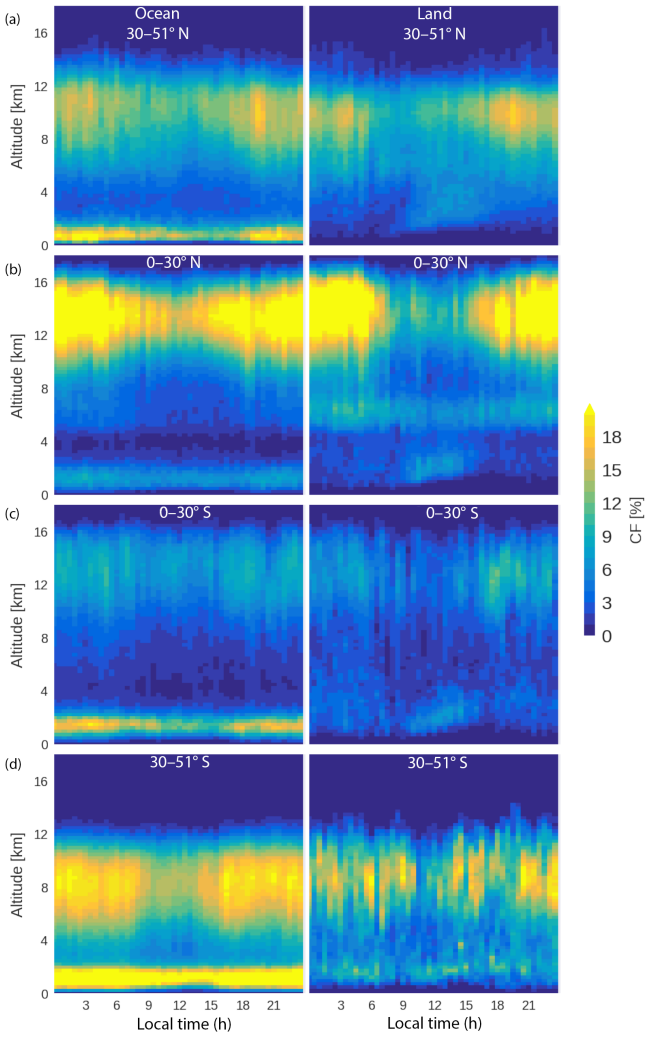

Figure 2. As in Fig. 1, over the Northern Hemisphere midlatitudes (row **a**) and tropics (row **b**) and over the Southern Hemisphere tropics (row **c**) and midlatitudes (row **d**) during JJA from 2015 to 2017.

3.2 Diurnal cloud fraction profiles observed over midlatitudes and tropics

In this section, we consider cloud populations over four latitude bands: midlatitude (30–51°) and tropics (0–30°) in the Northern Hemisphere (NH) and Southern Hemisphere (SH), over land and ocean. We first examine the differences between the diurnal cycles affecting the cloud vertical profiles over ocean and land in JJA (Sect. 3.2.1 and 3.2.2, Fig. 2), then we discuss how these cycles are affected by the season by considering DJF results (Sect. 3.2.3, Fig. 3).

3.2.1 High clouds

As expected, Fig. 2 shows that high clouds are located at higher altitude in the tropics (12–16 km a.s.l.) than in midlatitudes (8–12 km), following the variation of the troposphere depth with latitude. Also as expected, the occurrence of high clouds is largest (CF > 20 %) in deep convection along the Intertropical Convergence Zone (ITCZ), located between 0 and 30° N in JJA, and minimum (CF < 8 %) in the subsidence branch of the Hadley cell (0–30° S in JJA). In midlatitudes, high clouds (7–9 km a.s.l.) are far more frequent (CF ∼ 20 %) over the Southern Ocean (30–51° S) than over the NH midlatitude oceans (30–51° N).

The CF of oceanic high clouds follows a strong diurnal cycle, with a maximum at nighttime and a minimum at noon, in midlatitudes and tropics (even in the subsidence region). This cycle is more pronounced where the high clouds are more numerous: along the ITCZ (0–30° N) and in the Southern Ocean (30–51° S). In addition to the variation in the high cloud occurrence, the vertical distribution of these clouds also follows a marked diurnal cycle along the ITCZ: detec-

tions spread vertically over more than 4 km around midnight, but over less than 1 km at noon. This spreading occurs between 17:00 and 22:00 and disappears much faster during the morning. A wider spread of detection altitudes can either indicate the presence of geometrically thicker clouds or a wider distribution of optically thick cloud tops only partially sampled by CATS. By comparison, over the Southern Ocean high cloud detections occur over the same altitude range throughout the day.

Overall, high clouds behave very similarly above land (Fig. 2, right column) and ocean (Fig. 2, left column) at all latitudes, except between 30 and 51° S, where the continental surface is too small to conclude.

3.2.2 Low clouds

Over ocean in JJA (Fig. 2), the occurrence of low clouds (0–3 km a.s.l.) changes significantly with latitude: the Southern Ocean region (30–51° S) is by far the cloudiest, the midlatitude north (30–51° N) and the subsidence tropics (0–30° S) are moderately cloudy, and even less low clouds are observed along the ITCZ (0–30° N). The oceanic low clouds show only small variations along the day. A weak diurnal cycle occurs at all latitudes except along the ITCZ (possibly because low clouds there are in part masked by higher clouds affected by an out-of-phase diurnal cycle). Low-level clouds are more numerous in the nighttime (CF near 20 %) compared to daytime (CF ∼ 12 %) in the subsidence tropics (0–30° S) and midlatitude north (30–51° N). The southern oceanic low clouds exhibit a very faint diurnal cycle: their CF gets over 20 % nearly all day long, with a very small decrease around 14:00.

In contrast to high clouds, the differences between land and ocean are striking for the low- and mid-level clouds. Both the occurrences and the diurnal cycles of clouds over land differ significantly from their oceanic counterparts. The low clouds are very few over land (CF ∼ 4 %) compared to over ocean (> 16 %) all day long. Moreover, the continental low cloud diurnal cycle exhibits a maximum in the early afternoon (around 14:00) that does not show up over ocean: a maximum CF appears around 2.5 km of altitude in the upper edge (or just above the top) of the atmospheric boundary layer; it is linked to convective activity between 10:00 and 17:00.

Another noticeable difference between land and ocean is the presence of a well-defined mid-level cloud population over NH tropical land (0–30° N, second row on the right in Fig. 2) in the free troposphere between 5 and 7 km a.s.l. These mid-level clouds show a diurnal cycle opposite to PBL clouds and similar to the high clouds in that its minimum occurs at midday and its maximum at night, although the magnitude of this cycle is much more limited. This altitude range would be consistent with cumulus congestus clouds (Johnson et al., 1999). Those, however, are present above both land and ocean (Masugana et al., 2005) and CATS finds few clouds

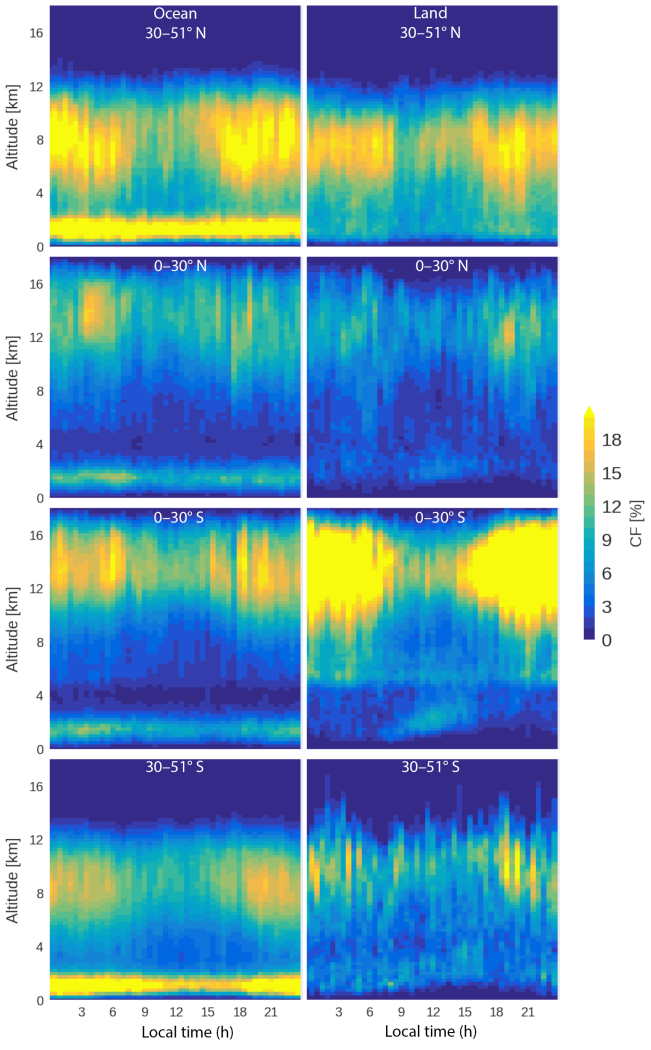

Figure 3. Same as Fig. 2, considering data CATS measured during the boreal winter (DJF, from 2015 to 2017).

at these altitudes over ocean. Rather, the cloud altitudes and location over land in the summer hemisphere are consistent with Altocumulus clouds as described by Sassen and Wang (2012) using CALIPSO and CloudSat measurements. Bourgeois et al. (2018) discussed the diurnal cycle of similar clouds observed over West Africa: they found these clouds reach maximum occurrence early in the morning, which is consistent with our results.

3.2.3 Seasonal differences

Figure 3 presents diurnal cycles of cloud fraction profiles over the same latitude bands as Fig. 2 but based on data collected during the boreal winter (DJF). As seasons switch hemispheres, we anticipate cloud populations to undergo symmetric changes across hemispheres, in agreement with large-scale dynamic processes driving their spatial distribution on seasonal timescales. This is verified for high clouds

(Fig. 2 vs. Fig. 3): in the tropics the ITCZ moves to the south and with it the large CF at high altitudes; in midlatitudes the high clouds are more frequent during the winter season, due to more frequent low-pressure conditions.

Interestingly, the mid-altitude clouds visible near 6 km a.s.l. in the NH tropics over land (Fig. 2, second row on the right) also move to the SH tropics in DJF (Fig. 3, third row on the right). This confirms the year-long persistence of midlevel clouds over continental tropical regions found by Bourgeois et al. (2018).

The seasonal changes in low clouds are less symmetric than in higher clouds, as they are more closely related to surface conditions. Over ocean, in DJF the amount of low clouds increases dramatically in NH midlatitudes compared to JJA (Figs. 2 and 3, top left), but does not change noticeably in the SH midlatitudes: the diurnal cycle that sees a slight decrease in the huge population of low clouds over the Southern Ocean is present in both seasons (Figs. 2 and 3, bottom left). Over land, in the tropics, low clouds appear similar in frequency and behavior in both DJF and JJA: PBL clouds extend vertically between ∼ 07:00 and 17:00 (Figs. 2 and 3, rows 2 and 3 of right column). The NH midlatitudes show the strongest seasonal change in low clouds, as they become present throughout the day: the diurnal cycle associated with PBL development in JJA disappears in DJF (Figs. 2 and 3, top right). SH midlatitude retrievals over land are noisy in DJF and JJA, but the DJF data (Fig. 3, bottom right) suggest that low clouds there extend vertically a lot more than in JJA, up to 4 km a.s.l.

3.3 Diurnal cycle of cloud profiles above selected continental regions

In this section, our first goal is to compare the diurnal cycle of the cloud fraction profiles from CATS against independent observations collected by active instruments from ground-based sites (Sect. 3.3.1 and 3.3.2). In particular, we want to understand if the behaviors found so far (Figs. 1–3) are valid for low clouds despite the attenuation of the space laser signal (Sect. 2.2.1). Our second goal is to compare, for the first time, the diurnal cycle of the cloud fraction profiles over different continental regions all over the globe as observed with a single instrument (Sect. 3.3.3).

It is important to note that since detection sensitivity, penetration depths, and algorithmic choices (e.g., averaging times and distances) change significantly from one instrument to the next, we do not expect the various datasets to agree on the absolute values of cloud fraction profiles or cloud amounts. Rather, our interest is in whether different instruments agree on the behavior of the diurnal evolution of clouds when they document the same location. Thus, the following comparison focuses on the main features of the daily cycles and not on absolute values.

3.3.1 Over the south of Paris in Europe

Figure 4 shows the diurnal evolution of CF profiles seen by the ground-based LNA lidar (top left) operated on the SIRTA site south of Paris (Sect. 2.1.2) and seen by CATS in a $10^\circ \times 10^\circ$ box centered on SIRTA, keeping only profiles sampled over land (top right). Both datasets report a well-defined high-altitude layer, with a clear-cut cloud top near 12 km a.s.l. that rises up a few hundred meters in the morning until 10:00 and slowly falls during the afternoon by at most 1 km. In both figures, the bottom of this layer is not sharply defined: the CF decreases almost linearly from 11 to 12 km a.s.l. to near-zero at 4 km a.s.l. Both instruments also report a low-level cloud layer that initiates in the morning and extends upwards from ∼ 1 km a.s.l. at 05:00 to ∼ 4 km a.s.l. around 20:00.

Regarding differences, CATS sees more high-altitude clouds. In the late afternoon (starting around 17:00), in particular, the ground-based lidar instead sees significantly fewer high clouds; that instrument, however, suffers from poor sampling at this late hour. CATS reports less boundary layer clouds, particularly in the late afternoon, when the ground-based lidar reports low-level CF above 20 % (again, a time of poor sampling). The large number of high-altitude clouds observed by CATS at that time could impair its ability to detect lower clouds, while at the same time the many low clouds observed by the ground lidar can impair its ability to detect high clouds. The absence of precipitating clouds from the LNA dataset could also explain this difference.

3.3.2 Over the US Southern Great Plains ARM site

Figure 4 shows the diurnal evolution of CF profiles seen by the SGP-based radar (second row, left) and CATS (right) in a $10^\circ \times 10^\circ$ latitude–longitude box centered on the SGP site (Sect. 2.2.2), keeping only profiles sampled over land. During nighttime, both datasets report frequent high-level clouds near 12 km a.s.l., with large CF between 16:00 and 03:00 LT. At night, high clouds are also more distributed vertically, between 9 and 14 km a.s.l. CATS and SGP datasets agree that the importance of high-level clouds strongly drops during daytime (07:00–17:00), with a minimum CF at midday. During daytime, the vertical distribution of high-level clouds is more narrow, from 11 to 12 km a.s.l. at its thinnest point (around 10:00). This rather strong cycle of high-level clouds can be explained by possible influence from tropical dynamics at the 36° N latitude of the SGP site. There are slightly more midlevel clouds (4–8 km a.s.l.) at night, with increasing CF between midnight, and 07:00 PBL clouds form near the surface at 09:00, rise, and thicken almost up to 4 km a.s.l. around 16:00.

There are of course differences. The SGP radar detects PBL and midlevel clouds twice as frequently as CATS, even though few high clouds are present. CATS also misses low-level clouds observed by the SGP radar between 18:00 and

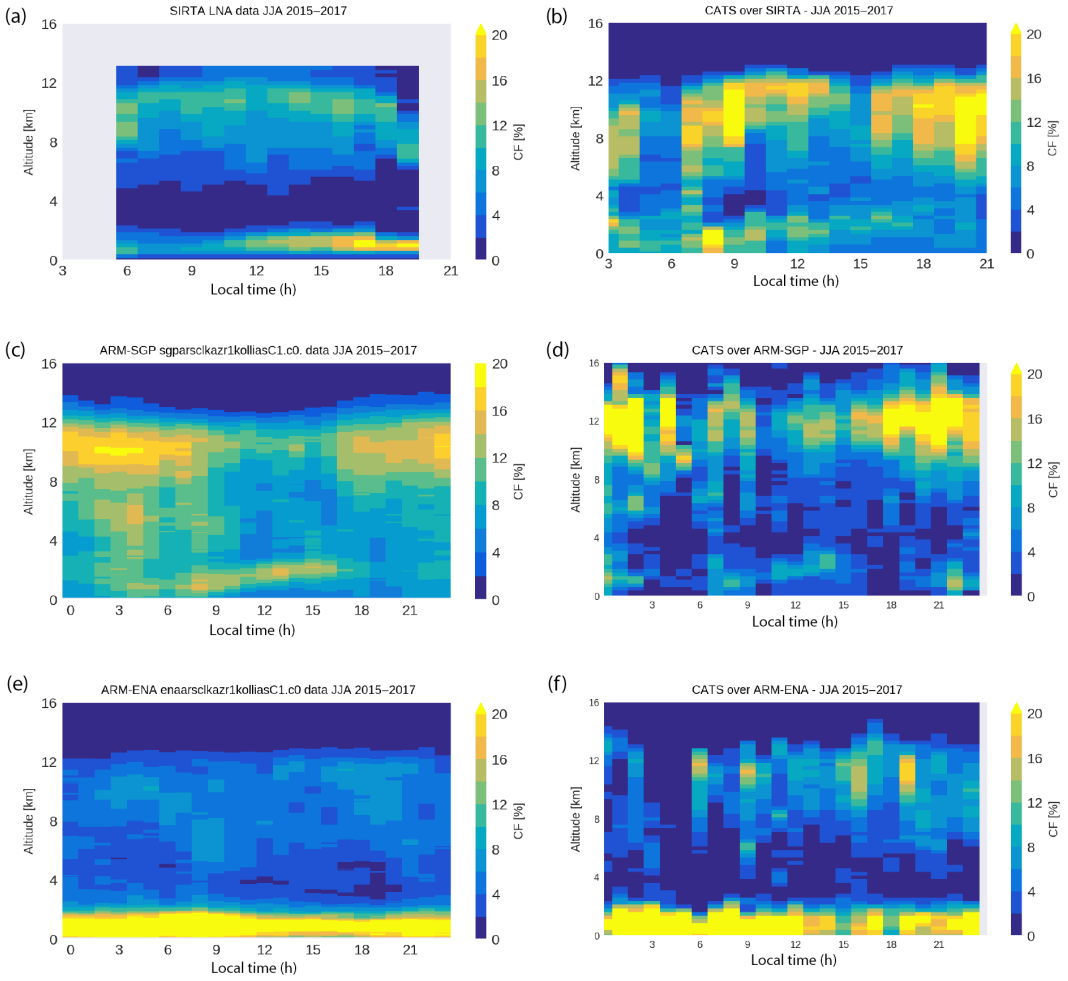

Figure 4. The diurnal cycle of cloud fraction profiles as seen by ground-based instruments (see text, **a, c, e**) and the CATS instrument **(b, d, f)** during JJA 2015–2017 at or in a 10° × 10° latitude–longitude box centered on **(a, b)** SIRTA, considering only sunlit conditions; **(c, d)** ARM-SGP; and **(e, f)** ARM-ENA. Times are local.

06:00, probably stratiform clouds that could either be too optically thin for CATS or miscategorized by its cloud detection algorithm.

3.3.3 Over the subtropical Eastern North Atlantic ARM site

Figure 4 shows the diurnal evolution of CF profiles seen by the ENA-based radar (bottom row, left) and CATS (right) in a 10° × 10° latitude–longitude box centered on the ENA site (Sect. 2.2.2). The vertical distribution of clouds appears very different over this oceanic site. Both CATS and the ENA radar agree on the day-long persistence of low-level clouds below 2 km a.s.l. and on their slight drop in cloud fraction and vertical spread between noon and 18:00. This is consistent with persistent stratiform clouds that are maximum at night. CATS sees more high clouds (8–12 km a.s.l.) than the ENA radar (4–12 km a.s.l.). CATS also reports a cloud fraction minimum between 03:00 and 05:00 LT that is not present in ground-based dataset.

These three comparisons between CATS and ground-based measurements suggest that, in general, the spaceborne lidar sees more high-level clouds and the ground-based instrument more low-level clouds. This sampling bias affects all space lidar comparisons with ground instruments (e.g., Dupont et al., 2010). Even so, we find similar behavior in the diurnal cycles reported by CATS and ground instruments over the same locations. Dataset discrepancies appear acceptable given the much smaller size of the CATS dataset (infrequent overpasses over three seasons compared to daily local measurements) and the instrumental and algorithmic variations already mentioned. It is reassuring to find that CATS results retain the major features of the cloud profile daily cycle, most notably an acceptable representation of the daytime low-level boundary layer clouds at all three sites despite the presence of high-level clouds.

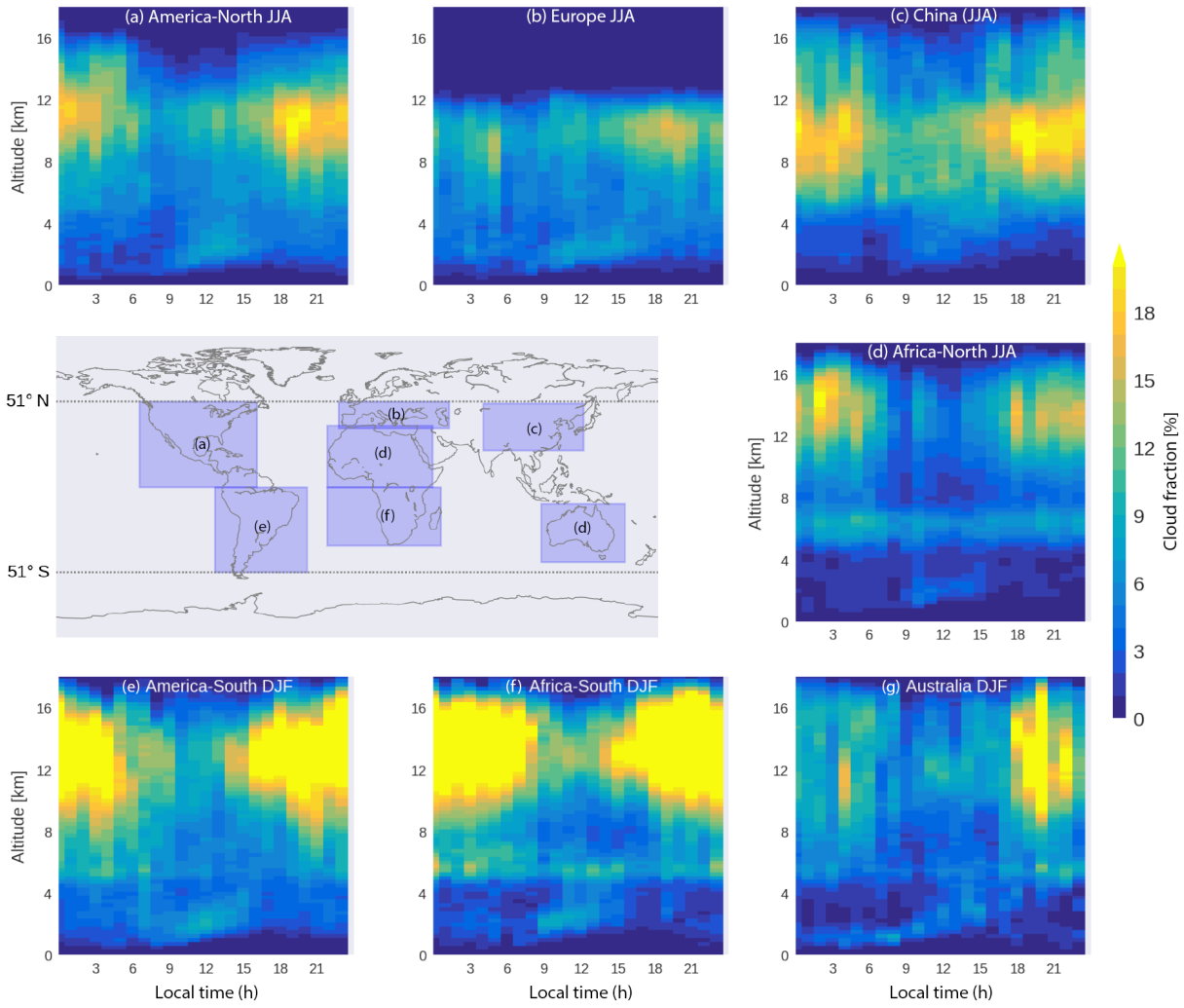

Figure 5. Diurnal cycle of the cloud fraction profiles observed by CATS over different continental regions – **(a)** NH America, **(b)** Europe, **(c)** China, **(d)** NH Africa, **(e)** SH America, **(f)** SH Africa, and **(g)** Australia – averaged over the summer months (JJA in the Northern Hemisphere and DJF in the Southern Hemisphere) from 2015 to 2017. For each region we considered all profiles sampled over land within the boundaries shown by the inset map. CFs over Europe do not extend to altitudes as high as the rest, as it is the only region that does not include part of the tropical band.

In this section, we have seen that retrievals from ground-based instruments suggest CATS measurements reliably document the cloud diurnal cycle. Due to the distribution of ground-based sites, however, this approach is limited to mostly midlatitudes from the Northern Hemisphere. Next, we compare CATS detections with global spaceborne retrievals.

3.3.4 Diurnal cycles of the cloud profiles over continents

Continents are diverse in ground type, orography, latitude, exposition to large-scale atmospheric circulation, and transport of air masses from the local environment. These factors influence the atmosphere above the continent, leading to possible variations in the cloud diurnal cycle profiles. Ground-based observations let us document these different cycles, but differences between instruments and operations in the different ground sites make comparing diurnal cycle observed from the ground at different locations difficult. Thanks to CATS data, for the first time we compare here the cloud diurnal cycle profiles observed over different continents by a single instrument and with a relatively large space sampling, compared to single-site ground-based observations. Figure 5 illustrates how the diurnal cycle of CF varies among seven large continental areas across both hemispheres, considering only cloud detections made by CATS over land within latitude–longitude boxes (defined in the inset map) during the summer seasons (JJA in the NH and DJF in the SH).

During summer most continents share a development of PBL clouds during sunlit hours (with similar cloud fractions, hours, and vertical extents), except NH Africa, where low clouds are almost absent. Most continents also share a nighttime maximum and daytime maximum of high clouds, with an associated narrowing of their vertical distribution during morning and a spreading during the afternoon. Variations in cloudiness and cloud vertical distribution are particularly intense over South America and SH Africa, while they are minimal over Australia. A mid-altitude cloud layer is present almost all day long, with a faint daytime minimum, over all SH continents and NH Africa.

Note that the present comparison is less robust in the lower troposphere than higher in the troposphere, due to the attenuation of the space lidar signal as it penetrates the atmosphere.

4 Discussion

Hereafter, we use our results for answering the following questions. How does the diurnal cycle of low, mid, and high cloud covers from geostationary satellites compare with CATS ones? Do the existing lidar space missions document extreme or average behaviors of the cloud profile diurnal cycle? What about upcoming sun-synchronous lidar space missions?

4.1 About the diurnal cycles of low and high cloud amounts

CATS observations provide an opportunity to compare the cloud diurnal cycle derived from the ISCCP dataset (Sect. 2.1.3) with completely independent observations on a near-global scale (excluding latitudes higher than 51°). In particular, we expect cloud retrievals from an active sensor such as CATS to be independent of the surface, even above highly reflective surfaces such as ice and deserts, and to include optically thin clouds. Since CATS sampling is constrained between 51° S and 51° N, its data cannot be used to document the diurnal cycle in the polar regions, like ISCCP does: our comparison will extend at most to midlatitudes. Figure 6 shows the diurnal cycle of the low and high cloud covers observed by the CATS space lidar.

Over ocean CAs are very stable and the diurnal cycle is almost flat (Fig. 6, left column). CATS shows a weak cycle for low clouds, with a maximum in mid-morning and a minimum in the early afternoon, which is also visible in ISCCP data. For oceanic high clouds, CATS exhibits almost no diurnal cycle except in the tropics where they follow the same cycle as low clouds. ISCCP also shows a weak cycle for high clouds, but opposite to the CATS one. This might be related to the fact that CATS can detect optically thin high clouds better than ISCCP. The optically thicker high clouds seen by ISCCP are thus probably more linked to deep convection activity. CATS can better detect optical thin high clouds, which should be more decoupled from convection and less affected by diurnal cycles.

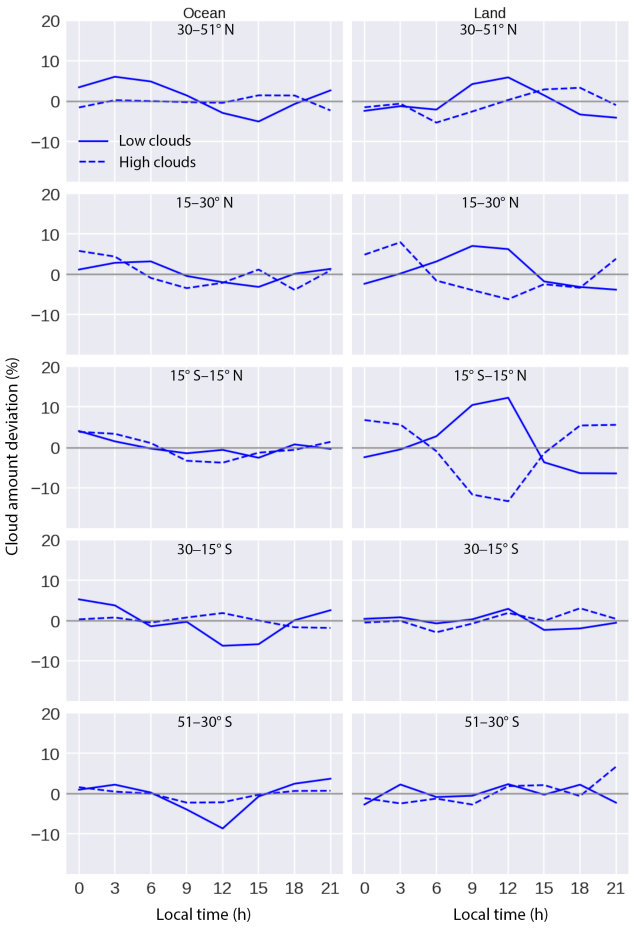

Figure 6. Mean diurnal variations of low-level (solid line) and high-level (dotted line) cloud amounts (%) every 3 h in five zonal bands over ocean (left) and land (right) in JJA from CATS for the period 2015–2017.

Over land, between 15° S and 51° N, CATS reports that low-level clouds have a pronounced diurnal cycle with a maximum of low-level clouds at midday (+10 %) and a minimum at midnight (−5 %). This is consistent with ISCCP observations (Fig. 11 in RS99), but in the northern midlatitudes the amplitude of the cycle is weaker for CATS than ISCCP (minimum at −4 % instead of −12 %). For high-level clouds over land in the tropics (15° S–30° N) CATS observes a maximum during nighttime and a minimum at noon; the timing is consistent with ISCCP but the amplitude is slightly more pronounced with CATS than ISCCP (−12 instead of −7 % at midday). In the Southern Hemisphere (15–51° S) the similarity between CATS and ISCCP is lost, probably because the land surface is small in those latitude ranges and the observations are not significant.

In summary, CATS confirms the shape of the low and high cloud diurnal cycles observed by ISCCP except for high trop-

ical clouds. This could be due to the space lidar detecting a larger number of optically thinner clouds not directly linked to deep convection, or to the different day–night cloud detection sensitivities of active and passive measurements. In most cases, the amplitudes of the diurnal cycle observed by CATS differ from those observed by ISCCP.

Both CATS and ISCCP miss some low clouds that are masked by the presence of high thick clouds. So even if CATS and ISCCP diurnal cycles are roughly consistent in low clouds, both results might be biased in the same direction. The high cloud diurnal cycles presented here are more robust than the low cloud ones.

4.2 About the cloud fraction profiles observed at fixed local times by space lidars

The CALIOP lidar has provided detailed cloud fraction profiles since 2006 at 01:30 and 13:30 LT. The next spaceborne atmospheric lidar mission ADM-Aeolus, to be launched in late 2018 (Culoma et al., 2017) on a sun-synchronous orbit, will enable measurements at 06:00 and 18:00 LT. After that, the atmospheric lidar (ATLID) on the EarthCARE platform (Illingworth et al., 2015), expected to launch in 2020, will operate at fixed local times close to CALIOP (02:00 and 14:00). The CATS dataset may remain for the near future our single source of diurnally distributed cloud profile lidar measurements from space.

4.2.1 Comparison between CATS and CALIPSO

In this section, we first check how CATS sees the day–night variation in cloud profiles also documented by CALIOP through its two daily overpasses. Figure 7 shows vertical profiles of cloud fraction reported by both datasets at 01:30 and 13:30, over ocean (left) and land (right), latitude weighted, and averaged between 51° S and 51° N over JJA between 2015 and 2017. The black lines show the CF obtained when considering all measurements from both instruments. Over land and ocean, we find that both CALIPSO and CATS overall report larger cloud fractions at 01:30 (blue) than 13:30 (red), in agreement with the findings of Gupta et al. (2018). Below 2.5 km, this difference is stronger over ocean (+7 % in the 01:30 CF) than over land. Both datasets report a strong increase in the 01:30 CF (almost +7 % compared to 13:30) above 15 km over land.

The CF profiles reported by both datasets agree very well over ocean (left) in both daytime and nighttime conditions. Over land (right) in daytime (red) conditions, CATS reports slightly more low-level clouds (CF ∼ 7 % near 1 km a.s.l., ∼ 5 % for CALIOP). This difference, which is present at all latitudes above land during daytime (not shown), might be due to the so-called single-shot low clouds, for which CALIOP data undergo a specific processing (Winker et al., 2009). The strongest differences appear for nighttime CF over land (right, blue): CALIPSO CF is larger than CATS

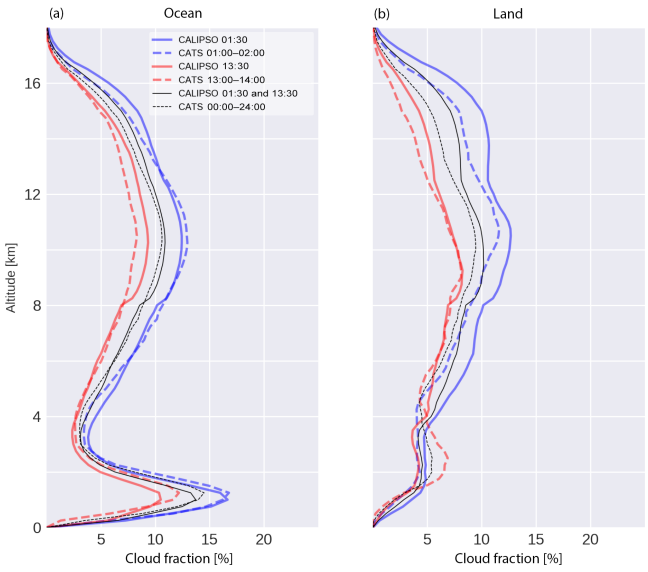

Figure 7. Vertical profiles of cloud fraction observed by CALIPSO (full line) and CATS (dashed line) between ±51° around 01:30 (blue), 13:30 (red), and at all times (black), over ocean **(a)** and land **(b)**. Measurements were weighted based on the latitude at which they were made to account for the different zonal sampling distributions of both instruments. CALIOP cloud profiles were built using cloud layers from the CALIPSO v4.10 level 2, 5 km cloud layer product. Only layers with a cloud–aerosol discrimination score (CAD_Score) above 0.7 were considered to build the CALIOP profiles, and layers with a Feature_Type_Score above 5 were considered to build the CATS profiles. For both instruments, we used JJA observations from 2015 to 2017.

CF by 2–3 % throughout the entire profile. A perfect agreement between CF from both datasets should not be expected, as the CATS and CALIOP lidars operate in different configurations – wavelengths, pulse repetition frequencies, and signal-to-noise ratios are different, for a start. These technical variations lead to differences in, for instance, how fast the laser pulse energy of both instruments gets attenuated as it penetrates atmospheres of various compositions, or differences in cloud detection performance, e.g., when sampling optically thin clouds in the upper troposphere, or fractionated boundary layer clouds (see Reverdy et al., 2015, for a study of the impact of design choices on lidar retrievals). Both datasets agree quite well on the general vertical pattern of the profile, though. A useful conclusion is that considering CALIPSO observations at both overpass local times (i.e., 01:30 and 13:30) apparently provides a good approximation of the daily average cloud fraction profile.

4.2.2 Comparison of cloud fraction profiles at various times of satellite overpass

As a final analysis, we represent the range covered by CATS hourly CF profiles over a day (averaged over the globe – white envelope in Fig. 8) and show CF profiles observed

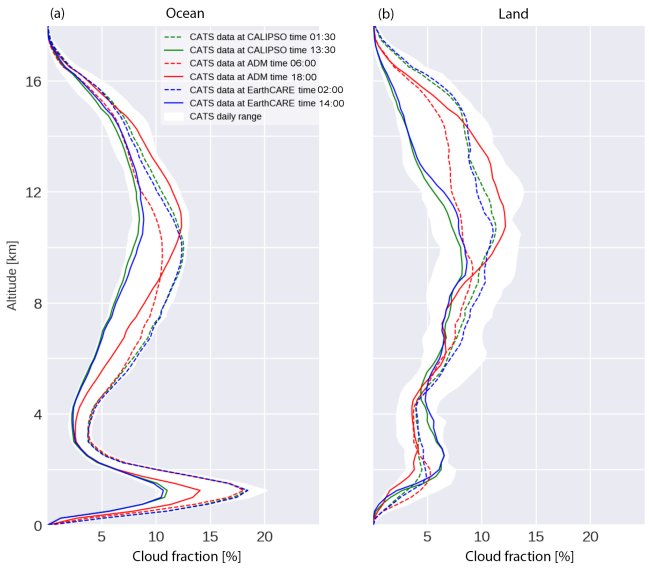

Figure 8. Mean cloud fraction profiles observed by CATS at the overpass local time of the sun-synchronous space lidars (CALIPSO and the A-Train 01:30 UTC, ADM 06:00 UTC, EarthCARE 02:00 UTC) compared to the envelope of the whole cloud fraction profile diurnal cycle observed by CATS (white), averaged between ±51° over ocean **(a)** and land **(b)**. CALIPSO and EarthCARE are dedicated to clouds and aerosols studies, while ADM is primarily dedicated to wind measurements in non-cloudy conditions. We used CATS observations during JJA from 2015 to 2017.

by CATS ± 1 h around the fixed local observation times of the three sun-synchronous space lidar missions (CALIPSO, ADM-Aeolus, EarthCARE).

Our first aim is to understand how wind observations made at fixed local time by ADM-Aeolus might be impacted by the cloud diurnal cycle. ADM-Aeolus will provide information on wind only in absence of clouds. Figure 8 indicates that ADM-Aeolus overpass times are quite cloudy in both nighttime and daytime compared to the diurnal variability (white envelope). The daytime overpass corresponds to the daily maximum in cloud profiles over both ocean and land, while nighttime observations correspond to a time representative of the daily average cloud fraction profile. As more clouds occur in the daytime than nighttime observations, less wind information will likely be provided by ADM-Aeolus in the afternoon than in the morning. For the future, another ADM-Aeolus-like mission around midday (minimum cloud fraction profile) would increase the number of wind measurements with respect to the cloud occurrence.

Our second aim is to understand how well observations made at fixed local times by space lidar dedicated to cloud studies (CALIPSO and EarthCARE) capture the daily variability of cloud fraction profiles. Figure 8 suggests that over land (right), CALIPSO and EarthCARE retrievals capture only part of the daily CF variability above 8 km a.s.l.: the daytime measurements overestimate the daily CF minima and the nighttime measurements underestimate the daily CF maxima. Below 8 km a.s.l. they are rather representative of the daily average, except below 5 km a.s.l., where daytime measurements get close to the daily CF maxima. Figure 8 also shows that over ocean (left), CALIPSO and EarthCARE retrievals should be considered as the daily CF maxima during the nighttime overpass and as the daily CF minima during the daytime overpass. This has interesting implications: it suggests that not only CALIPSO but all the observations dedicated to cloud studies collected by the instruments within the A-Train (CloudSat, CERES, MODIS, PARASOL, etc.) have documented the state of the atmosphere in the extreme states of the cloud profile diurnal cycle over the last 12 years over ocean. These conclusions suggest the A-Train observations are likely relevant and robust to constrain the cloud diurnal cycle extremes in climate models and climate studies.

5 Conclusions

In this paper, we took advantage of the variable local time of overpass of the International Space Station to document the diurnal cycle of the cloud vertical profile as seen by the CATS lidar. This is the first time the diurnal evolution of the vertical cloud profile is documented on that vertical scale on a large part of the globe, between 51° S and 51° N. Our results are based on 15 months of systematic observations (three boreal summers and two austral summers) collected during the 2015–2017 time period, which enable statistically significant results.

We observed that high tropical clouds begin to spread out vertically in the late afternoon (16:00–17:00). Their vertical distribution is largest (over 5 km) around 22:00. This spread is particularly large in the summer hemisphere in DJF. A mid-level cloud layer (4–8 km a.s.l.) persists all day long over the tropical continent during summer, with a weak diurnal cycle (minimum at noon). Southern Ocean results are quite unique; low clouds (0–2 km a.s.l.) cover this ocean all day long in summer and winter. A slight diurnal cycle sees their CF drop by a few percent during the afternoon (from noon to 18:00), but their vertical distribution stays constant. High clouds are also frequent over the Southern Ocean, more so in JJA. They follow a diurnal cycle in summer and winter, with a daytime minimum (from 08:00 to 15:00). At all latitudes, continental low clouds are most frequent in the early afternoon (around 14:00) at about 2.5 km a.s.l. Finally, our results show that in summer the diurnal cycle of continental clouds is similar in both hemispheres: a rapid development of near-surface PBL clouds during sunlit hours, and an increase in cloudiness and wider vertical distributions during nighttime for high-altitude clouds (stronger over the SH and the tropics). Exceptions are NH Africa, where PBL clouds are very few, and Australia, where high clouds appear only significant between 20:00 and 23:00.

We evaluated the diurnal cycle derived from CATS against independent ground-based observations and found satisfactory agreement. Moreover, our results suggest that over oceans CALIPSO and EarthCARE should describe the daily minimum of the cloud fraction profile during their daytime overpass and its daily maximum during their nighttime overpass. This supports the idea that data collected by A-Train instruments (not only CALIPSO) are very relevant to document the cloud diurnal cycle. This is also roughly the case over land at altitudes above 8 km a.s.l., although the amplitude of the diurnal variability is quite underestimated.

Questions remain about how several factors could affect our ability to retrieve the vertical variability of clouds from lidar-based measurements through the day. More specifically, the irruption of solar noise in daytime conditions requires increased horizontal averaging to keep the CATS detection sensitivity stable. High clouds with very small optical depths (lower than 0.005), which CATS can detect in the nighttime, will be probably missed in the daytime. Meanwhile, the occurrence and extent of fragmented boundary layer clouds might be overestimated. Even though prior work using the similarly affected CALIPSO data suggests the observed diurnal changes in clouds are too large to be solely due to those effects, their impact on the retrieved cycles needs to be quantified. In the same manner, how extinction by high clouds impacts the retrieved cloud fractions at low altitude needs to be investigated.

In the future, it would be possible to consider CATS measurements at smaller scales, to identify regionally consistent cloud populations and diurnal behaviors over specific regions of interest. It would also be possible to use CATS detection of opaque cloud layers to identify the best local time of observation from space to study local cloud radiative effects. We will address these lines of research in upcoming papers.

Data availability. The CALIPSO data were obtained from the online archive of the ICARE Data and Services Center: http://www.icare.univ-lille1.fr/archive (last access: 29 June 2018). The CATS data were obtained through the NASA Langley Research Atmospheric Science Data Center (ASDC): https://eosweb.larc.nasa.gov (last access: 29 June 2018). ARM-SGP and ARM-ENA data were obtained through the ARM portal: http://www.arm.gov (last access: 29 June 2018). SIRTA data were obtained through the ReOBS portal: http://sirta.ipsl.fr/reobs.html (last access: 29 June 2018).

Supplement. The supplement related to this article is available online at: https://doi.org/10.5194/acp-18-9457-2018-supplement.

Author contributions. VN, HC, MC and JY designed the study and figures. HC formulated the scientific questions investigated in Sect. 4.2. MC processed the SIRTA LNA data and provided expertise on its interpretation. JY provided expertise on the CATS data quality, processing, and interpretation. HC, MC, and JY contributed to the writing and editing. VN processed the CATS, CALIPSO, and ARM data, wrote the first draft, and produced the figures.

Competing interests. The authors declare that they have no conflict of interest.

Acknowledgements. Data were analyzed on the Climserv IPSL computing facilities. This research was made possible through support by CNRS and CNES. We want to thank Jean-Luc Baray and Nadège Montoux for useful discussions, as well as Pavlos Kollias and Karen Lee Johnson for help with ARM data.

Edited by: Matthias Tesche
Reviewed by: three anonymous referees

References

Bouniol, D., Roca, R., Fiolleau, T., and Poan, D. E.: Macrophysical, Microphysical, and Radiative Properties of Tropical Mesoscale Convective Systems over Their Life Cycle, J. Climate, 29, 3353–3371, https://doi.org/10.1175/JCLI-D-15-0551.1, 2016.

Bourgeois, E., Bouniol, D., Couvreux, F., Guichard, F., Marsham, J. H., Garcia-Carreras, L., Birch, C. E., and Parker, D. J.: Characteristics of mid-level clouds over West Africa, Q. J. Roy. Meteor. Soc., 113, D04210, https://doi.org/10.1002/qj.3215, 2018.

Cesana, G. and Chepfer, H.: Evaluation of the cloud thermodynamic phase in a climate model using CALIPSO-GOCCP, J. Geophys. Res., 118, 7922–7937, https://doi.org/10.1002/jgrd.50376, 2013.

Cesana, G., Chepfer, H., Winker, D. M., Getzewich, B., Cai, X., Okamoto, H., Hagihara, Y., Jourdan, O., Mioche, G., Noel, V., and Reverdy, M.: Using in situ airborne measurements to evaluate three cloud phase products derived from CALIPSO, J. Geophys. Res.-Atmos., 121, 5788–5808, https://doi.org/10.1002/2015JD024334, 2016.

Chepfer, H., Bony, S., Winker, D., Cesana, G., Dufresne, J. L., Minnis, P., Stubenrauch, C. J., and Zeng, S.: The GCM-Oriented CALIPSO Cloud Product (CALIPSO-GOCCP), J. Geophys. Res., 115, D00H16, https://doi.org/10.1029/2009JD012251, 2010.

Chepfer, H., Cesana, G., Winker, D., Getzewich, B., and Vaughan, M.: Comparison of two different cloud climatologies derived from CALIOP Level 1 observations: the CALIPSO-ST and the CALIPSO-GOCCP, J. Atmos. Ocean. Tech., 30, 725–744, https://doi.org/10.1175/JTECH-D-12-00057.1, 2013.

Chiriaco, M., Bastin, S., Yiou, P., Haeffelin, M., Dupont, J.-C., Klenov, L., and Stéfanon, M.: European heat-wave in July 2006: observations and modelling showing how local processes amplify conducive large-scale conditions, Geophys. Res. Lett., 41, 5644–5652, 2014.

Chiriaco, M., Dupont, J.-C., Bastin, S., Badosa, J., Lopez, J., Haeffelin, M., Chepfer, H., and Guzman, R.: ReOBS: a new approach to synthesize long-term multi-variable dataset and application to the SIRTA supersite, Earth Syst. Sci. Data, 10, 919–940, https://doi.org/10.5194/essd-10-919-2018, 2018.

Culoma, A., Elfving, A., Meynart, R., Straume, A., and Wernham, D.: AEOLUS mission: the latest preparations before launch,

Proc. SPIE 10423, Sensors, Systems, and Next-Generation Satellites XXI, 1042303, https://doi.org/10.1117/12.2282159, 2017.

Dong, X., Xi, B., Crosby, K., Long, C. N., Stone, R. S., and Shupe, M. D.: A 10 year climatology of Arctic cloud fraction and radiative forcing at Barrow, Alaska, J. Geophys. Res., 115, D17212, https://doi.org/10.1029/2009JD013489, 2010.

Dupont, J. C., Haeffelin, M., Morille, Y., Noel, V., Keckhut, P., Winker, D., Comstock, J., Chervet, P., and Roblin, A.: Macrophysical and optical properties of midlatitude cirrus clouds from four ground-based lidars and collocated CALIOP observations, J. Geophys. Res., 115, D00H24, https://doi.org/10.1029/2009JD011943, 2010.

Dupont, J.-C., Haeffelin, M., Morille, Y., Comstock, J. M., Flynn, C., Long, C. N., Sivaraman, C., and Newson, R. K.: Cloud properties derived from two lidars over the ARM SGP site, Geophys. Res. Lett., 38, L08814, https://doi.org/10.1029/2010GL046274, 2011.

Eastman, R. and Warren, S. G.: Diurnal Cycles of Cumulus, Cumulonimbus, Stratus, Stratocumulus, and Fog from Surface Observations over Land and Ocean, J. Climate, 27, 2386–2404, https://doi.org/10.1175/JCLI-D-13-00352.1, 2014.

Elouragini, S. and Flamant, P. H.: Iterative method to determine an averaged lidar ratio and the range resolved extinction in cirrus, Appl. Optics, 35, 1512–1518, 1996.

Gray, W. M. and Jacobson, R. W.: Diurnal variation of deep cumulus convection, Mon. Weather Rev., 105, 1171–1188, https://doi.org/10.1175/1520-0493(1977)105<1171:DVODCC>2.0.CO;2, 1977.

Greenwald, T. J. and Christopher, S. A.: Daytime variation of marine stratocumulus microphysical properties as observed from geostationary satellite, Geophys. Res. Lett., 26, 1723–1726, https://doi.org/10.1029/1999GL900346, 1999.

Gupta, A. K., Rajeev, K., Sijikumar, S., and Nair, A. K. M.: Enhanced daytime occurrence of clouds in the tropical upper troposphere over land and ocean, Atmos. Res., 201, 133–143, 2018.

Guzman, R., Chepfer, H., Noel, V., Vaillant de Guélis, T., Kay, J. E., Raberanto, P., Cesana, G., Vaughan, M. A., and Winker, D. M.: Direct atmosphere opacity observations from CALIPSO provide new constraints on cloud-radiation interactions, J. Geophys. Res., 122, 1066–1085, https://doi.org/10.1002/2016JD025946, 2017.

Haeffelin, M., Barthès, L., Bock, O., Boitel, C., Bony, S., Bouniol, D., Chepfer, H., Chiriaco, M., Cuesta, J., Delanoë, J., Drobinski, P., Dufresne, J.-L., Flamant, C., Grall, M., Hodzic, A., Hourdin, F., Lapouge, F., Lemaître, Y., Mathieu, A., Morille, Y., Naud, C., Noël, V., O'Hirok, W., Pelon, J., Pietras, C., Protat, A., Romand, B., Scialom, G., and Vautard, R.: SIRTA, a ground-based atmospheric observatory for cloud and aerosol research, Ann. Geophys., 23, 253–275, https://doi.org/10.5194/angeo-23-253-2005, 2005.

Haynes, J. M., Vonder Haar, T. H., L'Ecuyer, T., and Henderson, D.: Radiative heating characteristics of earth's cloudy atmosphere from vertically resolved active sensors, Geophys. Res. Lett., 40, 624–630, https://doi.org/10.1002/grl.50145, 2013.

Hoareau, C., Keckhut, P., Noel, V., Chepfer, H., and Baray, J.-L.: A decadal cirrus clouds climatology from ground-based and spaceborne lidars above the south of France (43.9° N–5.7° E), Atmos. Chem. Phys., 13, 6951–6963, https://doi.org/10.5194/acp-13-6951-2013, 2013.

Hogan, R. J., Illingworth, A. J., O'Connor, E. J., and Poiares Baptista, J. P. V.: Characteristics of mixed-phase clouds. II: A climatology from ground-based lidar, Q. J. Roy. Meteor. Soc., 129, 2117–2134, 2003.

Hu, Y., Winker, D., Vaughan, M., Lin, B., Omar, A., Trepte, C., Flittner, D., Yang, P., Nasiri, S. L., Baum, B., Holz, R., Sun, W., Liu, Z., Wang, Z., Young, S., Stamnes, K., Huang, J., and Kuehn, R.: CALIPSO/CALIOP Cloud Phase Discrimination Algorithm, J. Atmos. Ocean. Tech., 26, 2293–2309, 2009.

Illingworth, A. J., Barker, H. W., Beljaars, A., Ceccaldi, M., Chepfer, H., Clerbaux, N., Cole, J., Delanoë, J., Domenech, C., Donovan, D. P., Fukuda, S., Hirakata, M., Hogan, R. J., Huenerbein, A., Kollias, P., Kubota,T., Nakajima, T., Nakajima, T. Y., Nishizawa, T., Ohno, Y., Okamoto, H., Oki, R., Sato, K., Satoh, M., Shephard, M. W., Velázquez-Blázquez, A., Wandinger, U., Wehr, T., and van Zadelhoff, G.: The EarthCARE Satellite: The Next Step Forward in Global Measurements of Clouds, Aerosols, Precipitation, and Radiation, B. Am. Meteorol. Soc., 96, 1311–1332, https://doi.org/10.1175/BAMS-D-12-00227.1, 2015.

Johnson, R. H., Rickenbach, T. M., Rutledge, S. A., Ciesielski, P. E., and Schubert, W. H.: Trimodal Characteristics of Tropical Convection, J. Climate, 12, 2397–2418, https://doi.org/10.1175/1520-0442(1999)012<2397:TCOTC>2.0.CO;2, 1999.

Kato, S., Rose, F. G., Sun-Mack, S., Miller, W. F., Chen, Y., Rutan, D. A., Stephens, G. L., Loeb, N. G., Minnis, P., Wielicki, B. A., Winker, D. M., Charlock, T. P., Stackhouse Jr., P. W., Xu, K.-M., and Collins, W. D.: Improvements of top-of-atmosphere and surface irradiance computations with CALIPSO-, CloudSat-, and MODIS-derived cloud and aerosol properties, J. Geophys. Res., 116, D19209, https://doi.org/10.1029/2011JD016050, 2011.

Kollias, P., Bharadwaj, N., Widener, K., Jo, I., and Johnson, K.: Scanning ARM Cloud Radars. Part I: Operational Sampling Strategies, J. Atmos. Ocean. Tech., 31, 569–582, https://doi.org/10.1175/JTECH-D-13-00044.1, 2014.

Konsta, D., Dufresne, J. L., Chepfer, H., Idelkadi, A., and Cesana, G.: Use of A-train satellite observations (CALIPSO–PARASOL) to evaluate tropical cloud properties in the LMDZ5 GCM, Clim. Dynam., 47, 1263–1284, https://doi.org/10.1007/s00382-015-2900-y, 2016.

Kummerow, C., Barnes, W., Kozu, T., Shiue, J., and Simpson, J.: The Tropical Rainfall Measuring Mission (TRMM) sensor package, J. Atmos. Ocean. Tech., 15, 809–817, 1998.

L'Ecuyer, T. S. and Jiang, J. H.: Touring the atmosphere aboard the A-Train, Phys. Today, 63, 36–40, 2010.

L'Ecuyer, T. S., Wood, N. B., Haladay, T., Stephens, G. L., and Stackhouse Jr., P. W.: Impact of clouds on atmospheric heating based on the R04 CloudSat fluxes and heating rates data set, J. Geophys. Res., 113, D00A15, https://doi.org/10.1029/2008JD009951, 2008.

Liu, C. and Zipser, E. J.: Diurnal cycles of precipitation, clouds, and lightning in the tropics from 9 years of TRMM observations, Geophys. Res. Lett., 35, L04819, https://doi.org/10.1029/2007GL032437, 2008.

Liu, Z., Vaughan, M. A., Winker, D., Kittaka, C., Getzewich, B., Kuehn, R., Omar, A., Powell, K. A., Trepte, C., and Hostetler, C.: The CALIPSO lidar cloud and aerosol discrimination: Version 2 algorithm and initial assessment of performance, J. Atmos. Ocean. Tech., 26, 1198–1213, 2009.

Masunaga, H., L'Ecuyer, T. S., and Kummerow, C. D.: Variability in the Characteristics of Precipitation Systems in the Tropical Pacific. Part I: Spatial Structure, J. Climate, 18, 823–840, https://doi.org/10.1175/JCLI-3304.1, 2005.

McGill, M. J., Yorks, J. E., Scott, V. S., Kupchock, A. W., and Selmer, P. A.: The Cloud-Aerosol Transport System (CATS): A technology demonstration on the International Space Station, Proc. SPIE 9612, Lidar Remote Sensing for Environmental Monitoring XV, 96120A, https://doi.org/10.1117/12.2190841, 2015.

Naud, C., Del Genio, A. D., Haeffelin, M., Morille, Y., Noel, V., Dupont, J.-C., Turner, D., Lo, C., and Comstock, J. M.: Thermodynamic phase profiles of optically thin midlatitude clouds and their relation to temperature, J. Geophys. Res., 115, D11202, https://doi.org/10.1029/2009JD012889, 2010.

Noel, V. and Haeffelin, M.: Midlatitude Cirrus Clouds and Multiple Tropopauses from a 2002–2006 Climatology over the SIRTA observatory, J. Geophys. Res., 112, D13206, https://doi.org/10.1029/2006JD007753, 2007.

Palm, S. P., Hlavka, D. L., Selmer, P., and Pauly, R.: the Cloud Aerosol Transport System (CATS) Data Product Catalog release 3.0, available at: https://cats.gsfc.nasa.gov/media/docs/CATS_Data_Products_Catalog.pdf (last access: 23 January 2018), 2016.

Pappalardo, G., Amodeo, A., Apituley, A., Comeron, A., Freudenthaler, V., Linné, H., Ansmann, A., Bösenberg, J., D'Amico, G., Mattis, I., Mona, L., Wandinger, U., Amiridis, V., Alados-Arboledas, L., Nicolae, D., and Wiegner, M.: EARLINET: towards an advanced sustainable European aerosol lidar network, Atmos. Meas. Tech., 7, 2389–2409, https://doi.org/10.5194/amt-7-2389-2014, 2014.

Philippon, N., de Lapparent, B., Gond, V., Sèze, G., Martiny, N., Camberlin, P., Cornu, G., Morel, B., Moron, V., Bigot, S., Brou, T., and Dubreuil, V.: Analysis of the diurnal cycles for a better understanding of the mean annual cycle of forests greenness in Central Africa, Agr. Forest Meteorol., 223, 81–94, https://doi.org/10.1016/j.agrformet.2016.04.005, 2016.

Protat, A., Delanoë, J., Plana-Fattori, A., May, P. T., and O'Connor, E. J.: The statistical properties of tropical ice clouds generated by the West African and Australian monsoons, from ground-based radar-lidar observations, Q. J. Roy. Meteor. Soc., 136, 345–363, https://doi.org/10.1002/qj.490, 2009.

Reverdy, M., Chepfer, H., Donovan, D., Noel, V., Cesana, G., Hoareau, C., Chiriaco, M., and Bastin, S.: An Earth-CARE/ATLID simulator to evaluate cloud description in climate models, J. Geophys. Res., 120, 11090–11113, https://doi.org/10.1002/2015JD023919, 2015.

Rossow, W. B.: Measuring cloud properties from space: A review, J. Climate, 2, 201–213, 1989.

Rossow, W. B. and Schiffer, R. A.: Advances in understanding clouds from ISCCP, B. Am. Meteorol. Soc., 80, 2261–2288, https://doi.org/10.1175/1520-0477(1999)080<2261:AIUCFI>2.0.CO;2, 1999.

Rozendaal, M. A., Leovy, C. B., and Klein, S. A.: An Observational Study of Diurnal Variations of Marine Stratiform Cloud, J. Climate, 8, 1795–1809, 1995.

Sassen, K. and Benson, S.: A midlatitude Cirrus Cloud Climatology from the Facility for Atmospheric Remote Sensing. Part II : microphysical properties derived from lidar depolarisation, J. Atmos. Sci., 58, 2103–2112, https://doi.org/10.1175/1520-0469(2001)058<2103:AMCCCF>2.0.CO;2, 2001.

Sassen, K. and Wang, Z.: The Clouds of the Middle Troposphere: Composition, Radiative Impact, and Global Distribution, Surv. Geophys., 33, 677–691, https://doi.org/10.1007/s10712-011-9163-x, 2012.

Sassen, K., Wang, Z., and Liu, D.: Cirrus clouds and deep convection in the tropics: Insights from CALIPSO and CloudSat, J. Geophys. Res., 114, D00H06, https://doi.org/10.1029/2009JD011916, 2009.

Sèze, G., Pelon, J., Derrien, M., Le Gléau, H., and Six, B.: Evaluation against CALIPSO lidar observations of the multi-geostationary cloud cover and type dataset assembled in the framework of the Megha-Tropiques mission, Q. J. Roy. Meteor. Soc., 141, 774–797, https://doi.org/10.1002/qj.2392, 2014.

Shang, H., Letu, H., Nakajima, T. Y., Wang, Z., Ma, R., Wang, T., Lei, Y., Ji, D., Li, S., and Shi, J.: Diurnal cycle and seasonal variation of cloud cover over the Tibetan Plateau as determined from Himawari-8 new-generation geostationary satellite data, Sci. Rep.-UK, 8, 1–8, https://doi.org/10.1038/s41598-018-19431-w, 2018.

Soden, B. J.: The diurnal cycle of convection, clouds, and water vapor in the tropical upper troposphere, Geophys. Res. Lett., 27, 2173–2176, https://doi.org/10.1029/2000GL011436, 2000.

Stephens, G., Winker, D., Pelon, J., Trepte, C., Vane, D., Yuhas, C., L'Ecuyer, T., and Lebsock, M.: CloudSat and CALIPSO within the A-Train: Ten Years of Actively Observing the Earth System, B. Am. Meteorol. Soc., 99, 569–581, https://doi.org/10.1175/BAMS-D-16-0324.1, 2018.

Stephens, G. L. and Kummerow, C. D.: The Remote Sensing of Clouds and Precipitation from Space: A Review, J. Atmos. Sci., 64, 3742–3765, https://doi.org/10.1175/2006JAS2375.1, 2007.

Stubenrauch, C. J., Chédin, A., Rädel, G., Scott, N. A., and Serrar, S.: Cloud Properties and Their Seasonal and Diurnal Variability from TOVS Path-B, J. Climate, 19, 5531–5553, https://doi.org/10.1175/JCLI3929.1, 2006.

Taylor, S., Stier, P., White, B., Finkensieper, S., and Stengel, M.: Evaluating the diurnal cycle in cloud top temperature from SEVIRI, Atmos. Chem. Phys., 17, 7035–7053, https://doi.org/10.5194/acp-17-7035-2017, 2017.

Tian, B., Soden, B. J., and Wu, X.: Diurnal cycle of convection, clouds, and water vapor in the tropical upper troposphere: Satellites versus a general circulation model, J. Geophys. Res., 109, D10101, https://doi.org/10.1029/2003JD004117, 2004.

Vaughan, M. A., Powell, K. A., Winker, D. M., Hostetler, C. A., Kuehn, R. E., Hunt, W. H., Getzewich, B. J., Young, S. A., Liu, Z., and McGill, M. J.: Fully Automated Detection of Cloud and Aerosol Layers in the CALIPSO Lidar Measurements, J. Atmos. Ocean. Tech., 26, 2034–2050, https://doi.org/10.1175/2009JTECHA1228.1, 2009.

Wang, Z. and Sassen, K.: Cloud type and macrophysical property retrieval using multiple remote sensors, J. Appl. Meteorol., 40, 1665–1682, 2001.

Wilson, A. M. and Barros, A. P.: Orographic Land–Atmosphere Interactions and the Diurnal Cycle of Low-Level Clouds and Fog, J. Hydrometeorol., 18, 1513–1533, https://doi.org/10.1175/JHM-D-16-0186.1, 2017.

Winker, D., Chepfer, H., Noel, V., and Cai, X.: Observational Constraints on Cloud Feedbacks: The Role of Active Satellite Sensors, Surv. Geophys., 38, 1483–1508, https://doi.org/10.1007/s10712-017-9452-0, 2017.

Winker, D. M., Vaughan, M. A., Omar, A., Hu, Y., and Powell, K. A.: Overview of the CALIPSO mission and CALIOP data processing algorithms, J. Atmos. Ocean. Tech., 26, 2310–2323, 2009.

Winker, D. M., Pelon, J., Coakley Jr., J. A., Ackerman, S. A., Charlson, R. J., Colarco, P. R., Flamant, P., Fu, Q., Hoff, R. M., Kittaka, C., Kubar, T. L., Le Treut, H., McCormick, M. P., Mégie, G., Poole, L., Powell, K., Trepte, C., Vaughan, M. A., and Wielicki, B. A.: The CALIPSO mission: A global 3D view of aerosols and clouds, B. Am. Meteorol. Soc., 91, 1211–1229, 2010.

Yin, J. and Porporato, A.: Diurnal cloud cycle biases in climate models, Nat. Commun., 8, 2269, https://doi.org/10.1038/s41467-017-02369-4, 2017.

Yorks, J. E., Hlavka, D. L., Hart, W. D., and McGill, M. J.: Statistics of Cloud Optical Properties from Airborne Lidar Measurements, J. Atmos. Ocean. Tech., 28, 869–883, https://doi.org/10.1175/2011JTECHA1507.1, 2011.

Yorks, J. E., McGill, M. J., Palm, S. P., Hlavka, D. L., Selmer, P. A., Nowottnick, E. P., Vaughan, M. A., Rodier, S. D., and Hart, W. D.: An overview of the CATS level 1 processing algorithms and data products, Geophys. Res. Lett., 43, 4632–4639, https://doi.org/10.1002/2016GL068006, 2016a.

Yorks, J. E., Palm, S. P., McGill, M. J., Hlavka, D. L., Hart, W. D., Selmer, P. A., and Nowottnick, E.: CATS Algorithm Theoretical Basis Document, Level 1 and Level 2 Data Products, release 1.2, available at: https://cats.gsfc.nasa.gov/media/docs/CATS_ATBD.pdf (last access: 13 February 2018), 2016b.

Yorks, J. E., Rodier, S. D., Nowottnick, E., Selmer, P. A., McGill, M. J., Palm, S. P., and Vaughan, M. A.: CATS Level 2 Vertical Feature Mask Algorithms and Data Products: An Overview and Initial Assessment, Atmos. Meas. Tech. Discuss., in preparation, 2018.

Zhao, W., Marchand, R., and Fu, Q.: The diurnal cycle of clouds and precipitation at the ARM SGP site: Cloud radar observations and simulations from the multiscale modeling framework, J. Geophys. Res., 122, 7519–7536, https://doi.org/10.1002/2016JD026353, 2017.